Biosensors and Bioelectronics 77 (2016) 1175–1182

Contents lists available at ScienceDirect

Biosensors and Bioelectronics

journal homepage: www.elsevier.com/locate/bios

Screen-printed carbon electrode-based electrochemical immunosensor for rapid detection of microalbuminuria

Jang-Zern Tsai [a], Ching-Jung Chen [b,*], Kalpana Settu [a,*], Yu-Feng Lin [a], Chien-Lung Chen [c,d], Jen-Tsai Liu [e,*]

[a] Department of Electrical Engineering, National Central University, Jhongli, Taiwan
[b] School of Electronic and Communication Engineering, University of Chinese Academy of Sciences, Beijing, China
[c] Department of Nephrology, Landseed Hospital, Taoyuan, Taiwan
[d] Department of Biomedical Sciences and Engineering, College of Health Sciences and Technology, National Central University, Jhongli, Taiwan
[e] College of Materials Sciences and Opto-electronics, University of Chinese Academy of Sciences, Beijing, China

ARTICLE INFO

Article history:
Received 8 September 2015
Received in revised form
27 October 2015
Accepted 2 November 2015
Available online 9 November 2015

Keywords:
Screen-printed carbon electrode
Immunosensor
Microalbuminuria
Chronoamperometry

ABSTRACT

A urinary microalbumin test is used to detect early signs of kidney damage in people who have a risk of chronic kidney disease, such as those with diabetes or hypertension. In this study, we developed a screen-printed carbon electrode-based immunosensor for the detection of microalbumin in urine. Anti-human albumin antibodies were immobilized on the screen-printed sensor surface by the covalent immobilization method. Cyclic voltammetry (CV) and scanning electron microscopy with an energy dispersive spectroscopical (SEM-EDS) analysis demonstrated that the modification process was well performed. Chronoamperometric (CA) electrochemical measurement technique was employed for the quantitative detection of albumin. The electrochemical measurements performed with some possible interfering compounds normally present in urine (ascorbic acid, uric acid, glucose and creatinine samples) demonstrated a high specificity and selectivity of this immunosensor in albumin detection. Under optimum conditions, the immunosensor can detect urinary albumin in a wide linear range from 10 μg/ml to 300 μg/ml with a detection limit of 9.7 μg/ml. The excellent performance of this immunosensor was confirmed by analyzing microalbumin in urine samples; the results were in good agreement with those obtained by the standard immunoturbidimetric method. The biosensor proposed herein is easy to prepare and can be used for low-cost, rapid, and sensitive screening of microalbuminuria. This approach provides a promising platform for developing clinical point-of-care diagnostic applications.

1. Introduction

Human serum albumin (HSA) is the most abundant protein in the circulatory system, which is synthesized and secreted by the liver for maintaining the osmotic pressure needed for proper distribution of body fluids between intravascular compartments and body tissues. In a healthy person, only a small amount of albumin (up to 30 mg/day) is excreted in urine (Datta and Dasgupta, 2009). In some adverse conditions, the renal albumin excretion rate may increase to raise the albumin level in the urine. Microalbuminuria refers to urinary albumin excretion of 30–300 mg/day from a 24-h urine collection, or 30–300 mg/l from a random or first morning spot urine collection (Chugh and Bakris, 2007; Ribera et al., 2006). Urinary albumin is an important clinical marker for renal and cardiovascular diseases (Newman et al., 2005). Diabetic nephropathy occurs in 20–40% of patients with diabetes and is the leading cause of end-stage renal disease (ESRD). Persistent albuminuria in the range of 30–300 mg/day (microalbuminuria) has been shown to be the earliest stage of diabetic nephropathy and is also a significant sign for cardiovascular diseases. If without early detection and treatment, microalbuminuria may progress to irreversible macroalbuminuria (> 300 mg/day) over a period of years. Therefore, routine screening to detect patients at risk of developing microalbuminuria is crucial to patient care.

Clinically, the concentration of albumin in urine has been measured by semiquantitative dipsticks or by various quantitative immunochemical methods such as immunoturbidimetry (IT), immunonephelometry (IN), enzyme-linked immunosorbent assay (ELISA), radioimmunoassay (RIA), chemiluminescence immunoassay (CLIA) and fluorescence immunoassay (FIA) (Aoyagi et al., 2001; Choi et al., 2004; Comper et al., 2004; Marre et al., 1987; Thakkar et al., 1997; Watts et al., 1986). Among these methods, RIA and ELISA are more sensitive and require a smaller

* Corresponding authors.
E-mail addresses: me2452858@gmail.com (C.-J. Chen), kalpusara@gmail.com (K. Settu), jentsai.liu@gmail.com (J.-T. Liu).

http://dx.doi.org/10.1016/j.bios.2015.11.002
0956-5663/

amount of antisera, but some of the reagents used in these two methods are harmful to human or environment. IT is simple and rapid, but it requires a large amount of antisera. CLIA has a good sensitivity, but it requires some expensive reagents. Moreover, these methods require a long reaction time, special equipment and reagents, multiple processing steps, or professional staff. In case of limited availability of specialized staff and instrumentation, the biosensors could be an ideal alternative tool for measuring the analyte in biological samples (Goyal et al., 2007; Goyal et al., 2008, 2010; Gupta et al., 2006; Jain et al., 2006; Omidfar et al., 2011).

A biosensor facilitating rapid albumin measurement with low cost and ease of usage by non-specialist personnel in the point-of-care unit would be desirable. Up to now, several biosensors have been developed for detection of albumin in urine (Fatoni et al., 2014; Li et al., 2013; Lai et al., 2010; Omidfar et al., 2011). Lai et al. (2010) proposed a nanobiosensor based on localized surface plasmon resonance (LSPR) for the detection of microalbumin. They immobilized anti-human albumin antibody onto silver nanoparticles and detected urinary albumin concentrations in the range of 1 ng/ml to 1 μg/ml. Omidfar et al. (Omidfar et al., 2011) developed a urinary albumin immunosensor based on a screen-printed carbon electrode modified by colloidal gold nanoparticles (AuNP) and poly vinyl alcohol (PVA). They detected albumin in a linear range of 2.5–200 μg/ml by employing differential pulse voltammetry and square wave voltammetry. Li et al. (2013) developed a urinary HSA detection assay with a self-made portable SPR biosensor based on the reflection light intensity interrogation. In their study, anti-HSA monoclonal antibody was immobilized onto the gold sensing area and a detection range of 1–100 μg/ml HSA was achieved.

Though a high sensitivity has been achieved with all these biosensors, their detection ability does not cover the entire range of microalbuminuria (30–300 μg/ml) without intricate sample dilution. Therefore, broadening the detection range to fully cover the range of microalbuminuria without sample dilution, besides raising the sensitivity, is also an important issue in developing microalbumin biosensors. Recently, the screen-printed carbon electrode with a porous structure has been reported to be able to increase the detection sensitivity due to the increased surface area for electrochemical reactions (Niu et al., 2012). In this study, we further exploit the porous carbon electrode to broaden the albumin detection range. Here we report a simple and sensitive electrochemical immunosensor based on carboxyl-enriched porous screen-printed carbon electrode (SPCE) for detecting urinary albumin in the range of microalbuminuria.

2. Materials and methods

2.1. Reagents

N-hydroxysulfosuccinimide (sulfo-NHS), 1-ethyl-3-(3-dimethylamino-propyl) carbodiimide hydrochloride (EDC), uric acid, creatinine, glucose, ascorbic acid, bovine serum albumin (BSA), human albumin, and the mouse anti-human albumin monoclonal antibody were purchased from Sigma-Aldrich Corp. (St. Louis, MO, USA). The analytical grade hydrochloric acid (HCl) was obtained from Avantor Performance Materials (Center Valley, PA, USA). Calcium carbonate ($CaCO_3$) was supplied by Formosa Plastics Corporation (Taipei, Taiwan). Polyvinyl chloride (PVC) substrate was obtained from Jan Yan Print Int'l Corporation (Taoyuan, Taiwan). Carbon paste was purchased from Gwent Electronic Materials Ltd. (Pontypool, UK). Deionized water (18.2 MΩ/cm) obtained from a Lotun ultrapure water purification system (Lotun Technic Co., Ltd., Taipei, Taiwan) and filtered through a 0.22-μm Millipak 40 Membrane (Millipore Corp., Bedford, MA, USA) was used in all the experiments.

2.2. Fabrication of screen-printed carbon paste electrodes (SPCE)

Firstly, 0.63 g $CaCO_3$ powder and 0.09 g stearic acid were well dispersed in a 5-ml volatile thinner and then mixed with 1.80 g of carbon paste by using an IKA RW 20 digital stirrer (IKA Works Inc., NC, USA). Then, the carbon paste containing $CaCO_3$ and stearic acid was used to print electrodes on a PVC substrate by utilizing a TY-300 FAT screen-printing machine (ATMA CHAMP Ent. Corp., Taipei, Taiwan). After being dried by an oven at 60 °C for 30 min, the electrodes were immersed in 1-M HCl for 1 h for the $CaCO_3$ to dissolve. Finally, the electrodes were rinsed with deionized water and dried in air for further use. An electrode thus formed was a carboxyl-enriched porous screen-printed carbon electrode (COOH-P-SPCE). For a contrastive morphological analysis with the COOH-P-SPCE, a bare SPCE was also made with the same method but from carbon paste without mixing with $CaCO_3$ powder and stearic acid.

2.3. Immobilization of anti-HSA antibody on the SPCE

Anti-human albumin antibody was covalently attached to stearic acid at the outer layer of the electrode through EDC–NHS chemistry. Firstly, the electrode was immersed for 15 min in a 10-mM phosphate buffer with pH 6.0 containing 2-mM EDC and 5-mM sulfo-NHS. Then a 10-mM phosphate buffer solution with pH 7.2 containing anti-HSA (8.8 μg/ml) was dropped onto the electrode surface, which was then left at 4 °C overnight. The time of the anti-HSA immobilization was optimized to 150 min (see Section 3.3). To block nonspecific binding sites, the anti-HSA-immobilized electrode was incubated with a phosphate buffer (10 mM, pH 7.2) containing 1% BSA for 1 hour at 4 °C. Then the modified electrode was rinsed with the phosphate buffer to remove the unbounded BSA from the electrode surface.

2.4. Surface morphology and composition analysis

The surface morphology of the COOH-P-SPCE and that of the bare SPCE were compared by observing with a scanning electron microscope (SEM, Model S-3500N, Hitachi Ltd., Tokyo, Japan). To verify the anti-HSA immobilization process, the morphology and composition of the electrode surface at different stages of immobilization were observed by SEM coupled with an energy dispersive X-ray spectroscope (EDS, Model EX-200, HORIBA Ltd., Kyoto, Japan) and X-ray photoelectron spectroscopy (XPS, Sigma Probe, Thermo VG Scientific, West Sussex, UK).

2.5. Electrochemical measurements

The basic study of electrode modification was carried out using cyclic voltammetry (CV) at a scan rate of 50 mV/s with a potential range of −1 to +1 V. Chronoamperometry (CA) was used for the measurement of albumin concentrations. The initial potential and step potential were 0.2 and 0.3 V, respectively, each with a duration time of 30 s. The standard human albumin solutions with the concentration ranging from 10 to 400 μg/ml were each prepared by mixing a 10-mM buffer solution of pH 7.2 with a proper amount of HSA. The specificity of the immunosensor to detect the albumin level in urine was tested against creatinine (4 g/l), glucose (0.3 g/l) and other electroactive interferences such as uric acid (1.5 g/l) and ascorbic acid (40 mg/l) that are generally found in the urine. All the electrochemical measurements were performed in the presence of 0.1 M potassium ferricyanide as a redox probe. The electrochemical measurement was carried out using an IM6-eX electrochemical workstation (ZAHNER-Elektrik GmbH & Co. KG,

a

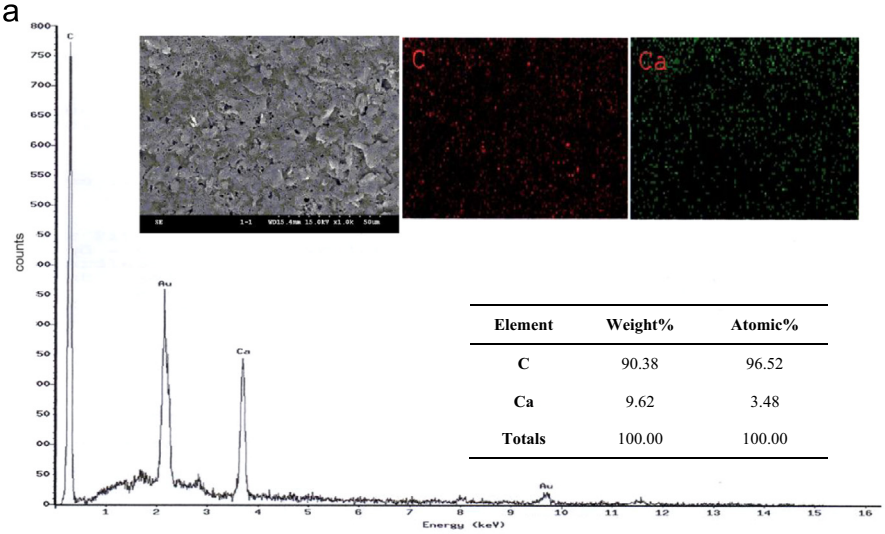

Element	Weight%	Atomic%
C	90.38	96.52
Ca	9.62	3.48
Totals	100.00	100.00

b

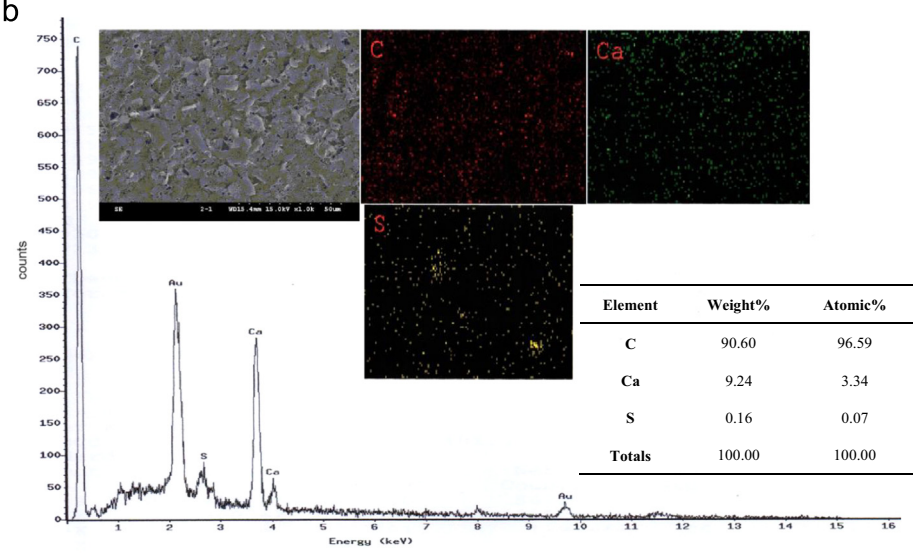

Element	Weight%	Atomic%
C	90.60	96.59
Ca	9.24	3.34
S	0.16	0.07
Totals	100.00	100.00

c

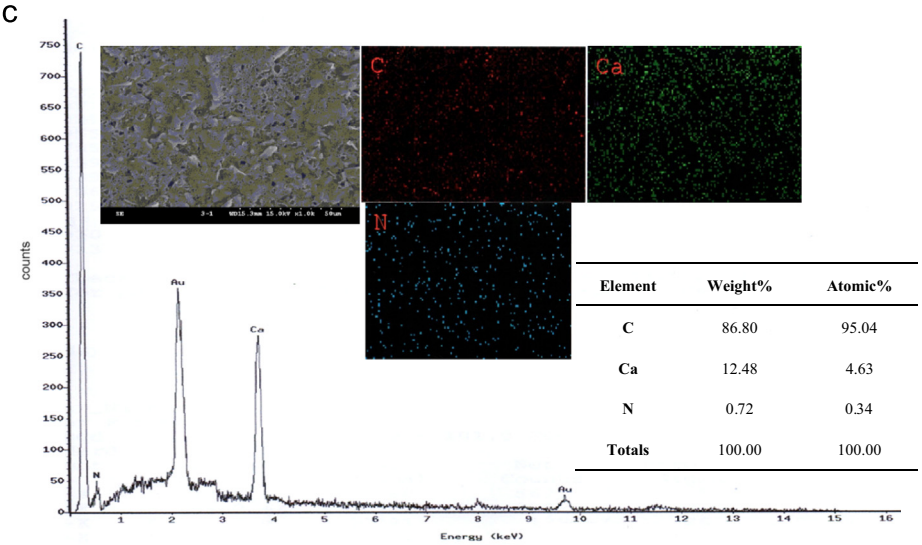

Element	Weight%	Atomic%
C	86.80	95.04
Ca	12.48	4.63
N	0.72	0.34
Totals	100.00	100.00

Fig. 1. SEM images (1000 ×) and EDS mapping analysis. (a) COOH-P-SPCE. (b) EDC–NHS/COOH-P-SPCE. (c) Anti-HSA/EDC–NHS/COOH-P-SPCE.

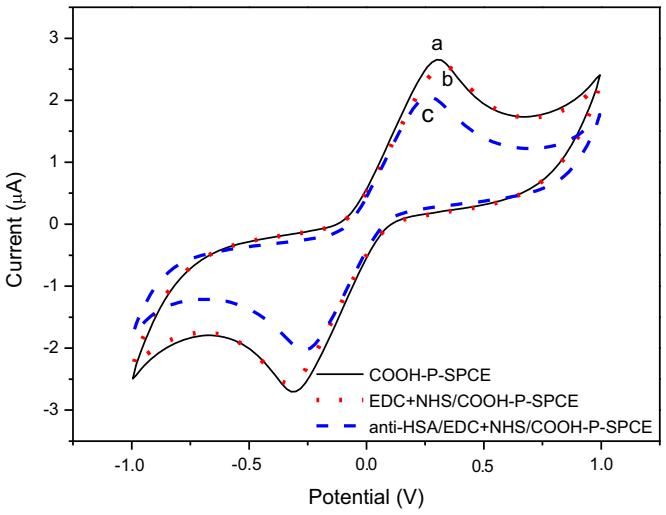

Fig. 2. The results of cyclic voltammetry following each immobilization step.

Germany). One contact pad of the screen-printed electrode was connected to the test and sense probes, and the other was connected to the reference and counter probes on the IM-6eX workstation.

2.6. Human urine samples preparation and analysis

Urine sample remains and microalbumin data were recruited from healthy persons and kidney disease patients, and disconnection of the identification of sample origins was done under an Institutional Review Board-approved protocol at Landseed hospital (Taoyuan, Taiwan). Each sample was centrifuged at 1500*g* for 5 min before the electrochemical measurements. Meanwhile, the albumin concentrations of these samples were confirmed with the standard clinical chemistry by immunoturbidimetry using MALB Flex reagent cartridges (Siemens Healthcare, New York, USA) in the hospital.

3. Results and discussion

3.1. Characterization of SPCE electrodes

SEM pictures were taken to compare the surface morphology of the COOH-P-SPCE with that of the bare SPCE. Fig. S1 (Supplementary material) reveals significant differences between them. The bare SPCE surface comprised relatively smooth carbon flakes, whereas the carbon flakes of the COOH-P-SPCE surface exhibited a great number of pores. The porous morphology of the COOH-P-SPCE surface could be attributed to the dissolution of $CaCO_3$ doped in the carbon paste. Due to the high CaCO3 doping ratio, a large amount of pores were formed and they linked together with deeply stretching channels. The porous structure exhibited a complex three-dimensional network with a large total surface area, which could enhance the detection sensitivity (Goyal et al., 2010; Niu et al., 2012).

Fig. S2a and b (Supplementary material) shows the C 1s peaks of the electrode surfaces of the bare SPCE and the COOH-P-SPCE, respectively, measured by XPS. The Origin-8 (OriginLab Corp., Northampton, MA, USA) software was used to fit the XPS spectra and to calculate elemental compositions from the peak areas. The peaks were fitted by using the Gaussian distribution function. The C 1s peak of the bare SPCE was at 284.6 eV that is ascribed to the graphitic carbon functional group (Polovina et al., 1997; Wang and Sherwood, 1994). The C 1s peak of the COOH-P-SPCE can be resolved into two individual peaks that are ascribed to graphitic carbon (284.6 eV) and carboxyl groups (287.25 eV), respectively (Molder et al., 1995). The weight content of the carboxyl group is estimated to be about 17.51% on the basis of the calculated area under the resolved peak at 287.25 eV (the blue dash–dot line in Fig. S2b). This result validates that the electrode prepared with stearic acid contained the carboxyl group, which enabled immobilization of antibody on the electrode surface.

3.2. Immunosensor characterization

3.2.1. SEM-EDS

Fig. 1a–c shows the results of energy dispersive spectroscopical analyses of COOH-P-SPCE surface before surface modification, after surface modification with EDC–NHS, and after surface modification with anti-HSA antibody, respectively. Fig. 1a indicates that the COOH-P-SPCE surface was composed of 90.38 wt% of carbon and 9.62 wt% of calcium. The presence of calcium element reflected the addition of calcium carbonate powder in the carbon paste for making the porous carbon structure. Fig. 1b indicates that, after being dropped with EDC and sulfo-NHS, the electrode surface contained sulfur along with carbon and calcium elements (90.60 wt% of C, 9.24 wt% of Ca, and 0.16 wt% of S). The presence of sulfur (from sulfo-NHS) on the electrode surface proved that the carboxyl groups on electrode surface were successfully activated by EDC/sulfo-NHS. Fig. 1c shows that, after being dropped with anti-HSA, the electrode surface consisted of 86.8 wt% of carbon, 12.48 wt% of calcium, and 0.72 wt% of nitrogen. The presence of nitrogen in the EDS result reflected successful immobilization of anti-HSA on the electrode surface. In all these cases, the SEM pictures and EDS mapping analyses showed the homogeneous distribution of elements over the sample surface, demonstrating the successful modification of electrode surface.

3.2.2. Cyclic voltammetry

Cyclic voltammetry experiments further confirmed that the EDC–NHS and antibody were successfully assembled on the COOH-P-SPCE surface. After the electrode surface is modified by some material, the electron transfer kinetics of $[Fe(CN)6]^{4-}$/$[Fe(CN)6]^{3-}$ is perturbed. Fig. 2 shows the average cyclic voltammograms of potassium ferricyanide at bare COOH-P-SPCEs (the solid curve, a), EDC–NHS-modified electrodes (the dotted curve, b) and antibody-immobilized electrodes (the dashed curve, c). As shown in Fig. 2, the assembly of antibody molecules on a COOH-P-SPCE electrode was accompanied by a decrease in the cyclic voltammetric response of the electrode. This was consistent with the enhanced electron transfer barriers introduced upon the assembly of this layer. It is usually assumed that the electron transfer of $[Fe(CN)6]^{4-}$/$[Fe(CN)6]^{3-}$ redox probe is blocked by formation of organized layers on the electrode surface because these redox species do not penetrate the layers into the conductive electrode surface. As shown in Fig. 2, the change in the oxidation peak was inconsiderable after the bare COOH-P-SPCE electrode was modified with EDC–NHS. Subsequently, after the immobilization of antibody (anti-HSA) onto the electrode surface, the oxidation peak obviously decreased to 2.054 μA from 2.654 μA of the bare COOH-P-SPCE electrode. The reason was that the immobilized antibody acted as an inert electron transfer blocking layer, and it hindered the diffusion of $[Fe(CN)6]^{4-}$/$[Fe(CN)6]^{3-}$ redox probe toward the electrode surface. This result proved the success in immobilizing antibodies onto the electrode surface.

3.3. Optimization of antibody immobilization and antigen binding times

The CV oxidation peak values were measured for the

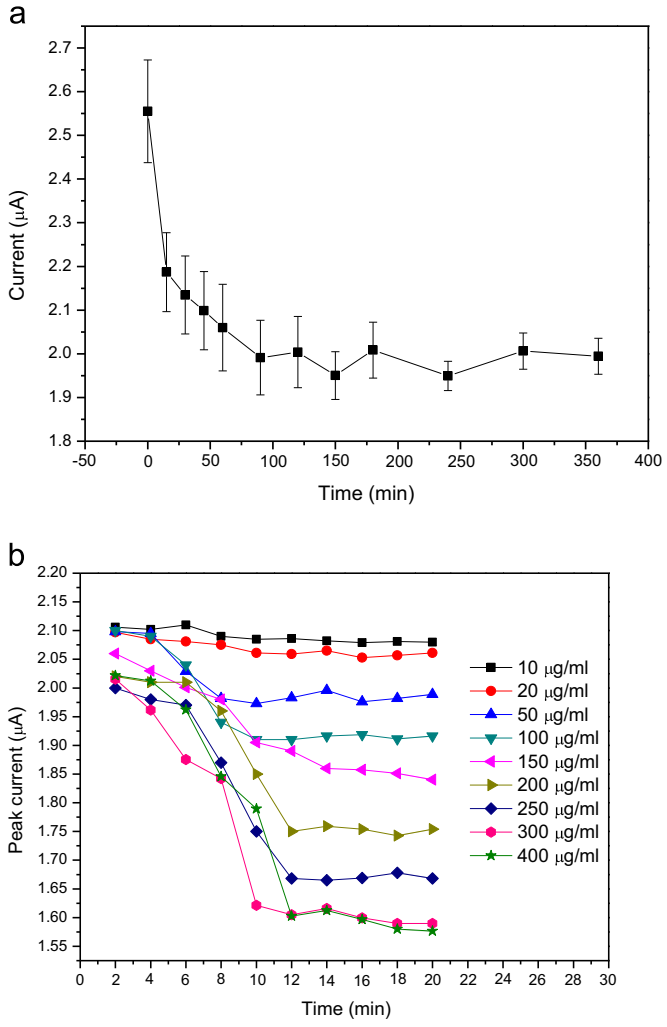

Fig. 3. Optimization of (a) Antibody (anti-HSA) immobilization time and, (b) HSA binding time.

optimization of anti-HSA immobilization time and HSA binding time. Fig. 3a illustrates the optimization of antibody immobilization time for the biosensor fabrication. The sensors for the optimization were fabricated with an anti-HSA solution of 8.8 μg/ml concentration and various lengths of immobilization time were used for the assay. The CV peak currents almost stabilized when the antibody immobilization time was higher than 150 min. Thus 150 min was chosen as the optimized immobilization time for the biosensor fabrication.

Fig. 3b shows the time optimization for HSA binding with anti-HSA. Anti-HSA-modified sensors each fabricated with an immobilization time of 150 min were used for the assay of various HSA concentrations (10–400 μg/ml). For each HSA concentration, different lengths (2, 4, …, 20 min) of reaction time for HSA binding were tried. As shown in Fig. 3b, the CV peak currents tended to level off when the reaction time increased beyond 14 min. Thus, 14 min was chosen as the optimized reaction time for sample assays. In Fig. 3, each data point represents the average value of five repetitive experiments. The error bars stand for standard deviations.

3.4. Interference study

After characterizing the modified electrodes with cyclic voltammetry, a detailed investigation was conducted using chronoamperometry to optimize detection potential, generate calibration data and apply the proposed method to real samples. Chronoamperometry was used instead of cyclic voltammetry because it is more sensitive, offers a higher signal-to-noise ratio, can conquer potential interferences in urine and, moreover, it is an easier detection method to implement (Dungchai et al., 2009; Goyal et al., 2007; Kanyong et al., 2012; Nie et al., 2010).

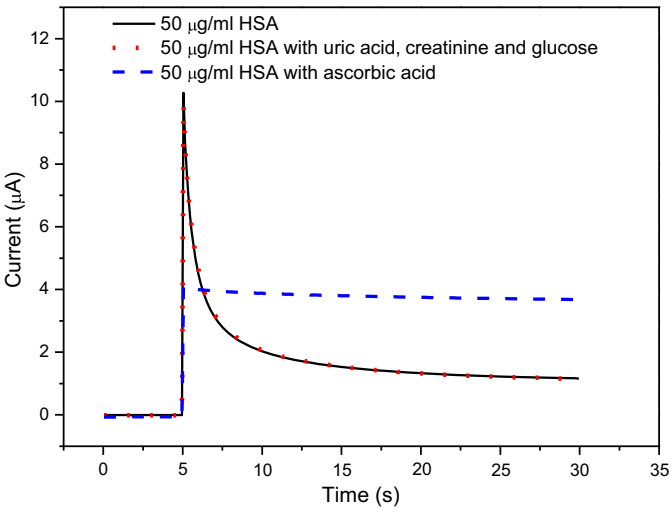

Fig. 4. Chronoamperograms of HSA with/without interferents.

First, chronoamperometry was performed by stepping from 0 V (for 5 s) to +0.3 V (for 25 s) for testing the selectivity of the proposed immunosensors. The interference study of the immunosensor was carried out by comparing the chronoamperometric response before and after adding some interferents such as uric acid (1.5 g/l), creatinine (4 g/l), glucose (0.3 g/l), and ascorbic acid (40 mg/l) along with 50-μg/ml HSA in a 10-mM phosphate buffer (pH 7.2) with 0.1-M $K_3[Fe(CN)_6]$. As shown in Fig. 4, the current response at 15 s was 2.02 and 2.01 μA for HSA without and with interferents (uric acid, creatinine and glucose), respectively. This result showed that uric acid, creatinine, and glucose have practically no interference. Whereas, increased current response of 3.8 μA was observed with ascorbic acid compared with other interferences as shown in Fig. 4. The excess current was due to the oxidation of ascorbic acid (Pournaghi-Azar and Ojani, 1995). $[Fe(CN)6]^{4-}$ has the ability to electrocatalyze the oxidation of ascorbic acid via a homogeneous process when the ferrocyanide is present in the dissolved form (Winograd et al., 1969). In this study, we used 0.1-M $K_3[Fe(CN)_6]$ as the redox probe in the dissolved form and hence the increase in the current response with ascorbic acid was from the oxidation of ascorbic acid. The oxidation current almost stayed constant at about 4 μA without decay (Fig. 4, the dashed curve) and this could be due to the electrode fouling caused by ascorbic acid. In HSA detection, the oxidation ability of ascorbic acid in the presence of ferricyanide can cause interference and become a critical problem. In order to eliminate the oxidation effect of ascorbic acid during HSA detection, we decided to oxidize the ascorbic acid prior to HSA detection. According to the work proposed by Lin et al. (2004), ascorbic acid could be oxidized at the potential of +0.2 V. Considering the ascorbic acid oxidation potential, we conducted chronoamperometry with an initial potential of +0.2 V for 30 s for oxidizing the ascorbic acid to reduce electrode fouling followed by a step potential of +0.30 V for 30 s for the detection of HSA. Ascorbic acid was oxidized at the potential of +0.2 V and hence the interfering effect from ascorbic acid was successfully eliminated in HSA detection (See Section

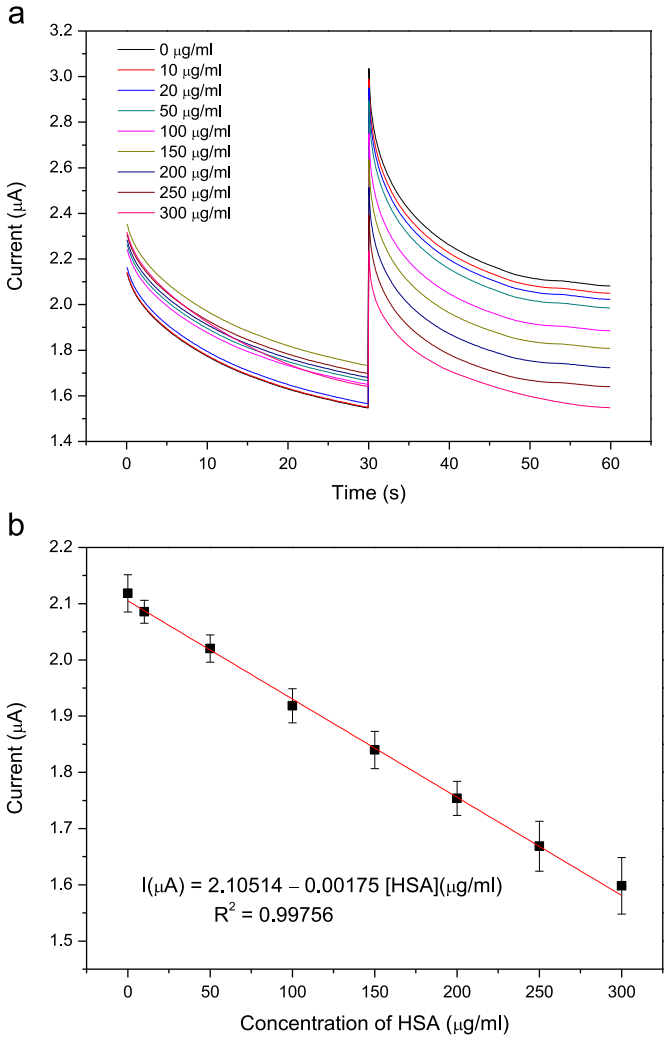

Fig. 5. (a) The chronoamperometric response with various concentrations of HSA. (b) The relationship between the current magnitude of the chronoamperometric response at 50 s and the HSA concentration.

3.5).

3.5. Detection of HSA

A calibration curve would be obtained with known amounts of HSA in the presence of uric acid (1.5 g/l), creatinine (4 g/l), glucose (0.3 g/l), and ascorbic acid (40 mg/l). Fig. 5a depicts the chronoamperometric responses of the HSA immunosensor with HSA concentrations ranging from 0 to 300 μg/ml. The binding interaction between HSA and the immobilized anti-HSA on the electrode surface caused the current response to decrease with increasing HSA concentrations, as can be seen from Fig. 5a. The amperometric response at 50 s was chosen for the detection of HSA concentration and the cuurent magnitude at that instant with respect to the corresponding HSA concentration is plotted in Fig. 5b. The amperometric response of the HSA immunosensor exhibited a linear relationship with the HSA concentrations ranging from 10 to 300 μg/ml, and the linear equation was I (μA)=2.10514−0.00175 [HSA] (μg/ml) with a coefficient of determination R^2=0.997. The limit of detection was calculated according to the $3s_a/b$ criterion, where b was the slope of the calibration curve, and s_a was the estimated standard deviation of the y-intercepts of the regression line (Jain et al., 2010; Sanagi et al., 2009). The detection limit calculated was 9.77 μg/ml. As seen from Fig. 5b, the linear part of the calibration curve includes the microalbumin range, from 30 to 300 μg/ml. Thus, this study could offer a simple approach for clinical microalbumin measurement, with disposable screen-printed electrodes.

3.6. Application of optimum immunosensor for the determination of microalbuminuria in human

Experiments were conducted to evaluate the proposed immunosensor's performance in measuring albumin in real urine. The albumin concentrations measured with the immunoturbidimetry method were used as the gold standards. The urine samples were collected from 29 renal disease patients as well as from 3 healthy donors. Five individual immunosensors were used for each assay and the relative standard deviations (RSDs) of the measurement results were less than 6%. Fig. 6a shows the relationship between the albumin concentrations measured by the proposed immunosensor and the gold standards. The linear regression analysis resulted in a slope of 0.988 and a coefficient of determination R^2=0.99. The Bland–Altman plot was used to assess the interchangeability of the proposed immunosensor with the immunoturbidimetry method (Bland and Altman, 1986). As shown in Fig. 6b, the proposed immunosensor had a small bias (the mean difference between immunosensor and immunoturbidimetry) of −1.4 μg/ml, and the range between the two limits of agreement (mean−1.96 SD and mean+1.96 SD, i. e., −20.6 and 17.8 μg/ml) was sufficiently small, suggesting good consistency and clinical compatibility between these two methods. Hence we can assume that these two methods are interchangeable (Petersen et al., 1997; Tholance et al., 2011). In addition, the proposed immunosensor is more facile and spends only 15 min to acquire the albumin concentration in a urine sample. In summary, the proposed electrochemical immunosensor showed a great promise for microalbuminuria detection in real urine samples and could find valuable applications in the clinical setting.

4. Conclusion

In this study, we have developed a simple electrochemical immunosensor based on the carboxyl porous screen-printed carbon electrode (COOH-P-SPCE) for quantitative measurement of microalbumin in urine. The electrode was made of carbon paste mixed with calcium carbonate and stearic acid; this strategy offers a facile and low-cost route to mass-produce sensitive biosensing electrodes. To the best of our knowledge, our proposed immunosensor is the simplest one for microalbumin measurement. This immunosensor is used in conjunction with chronoamperometry to attain rapid and highly selective albumin detection with minimized interference from the oxidation of ascorbic acid. High reproducibility of the detection was confirmed using urine samples from patients as well as healthy controls. The performance of this immunosensor in urine sample microalbumin detection showed a good agreement with the standard immunoturbidimetric method generally used in hospitals. The cost of the proposed immunosensor plus that of the associated electrochemical apparatus is much lower than that of the immunoturbidimetric measurement apparatus. The proposed immunosensor is suitable for point-of-care applications and it can detect microalbumin (30–300 μg/ml) in urine, which is important for clinical diagnosis.

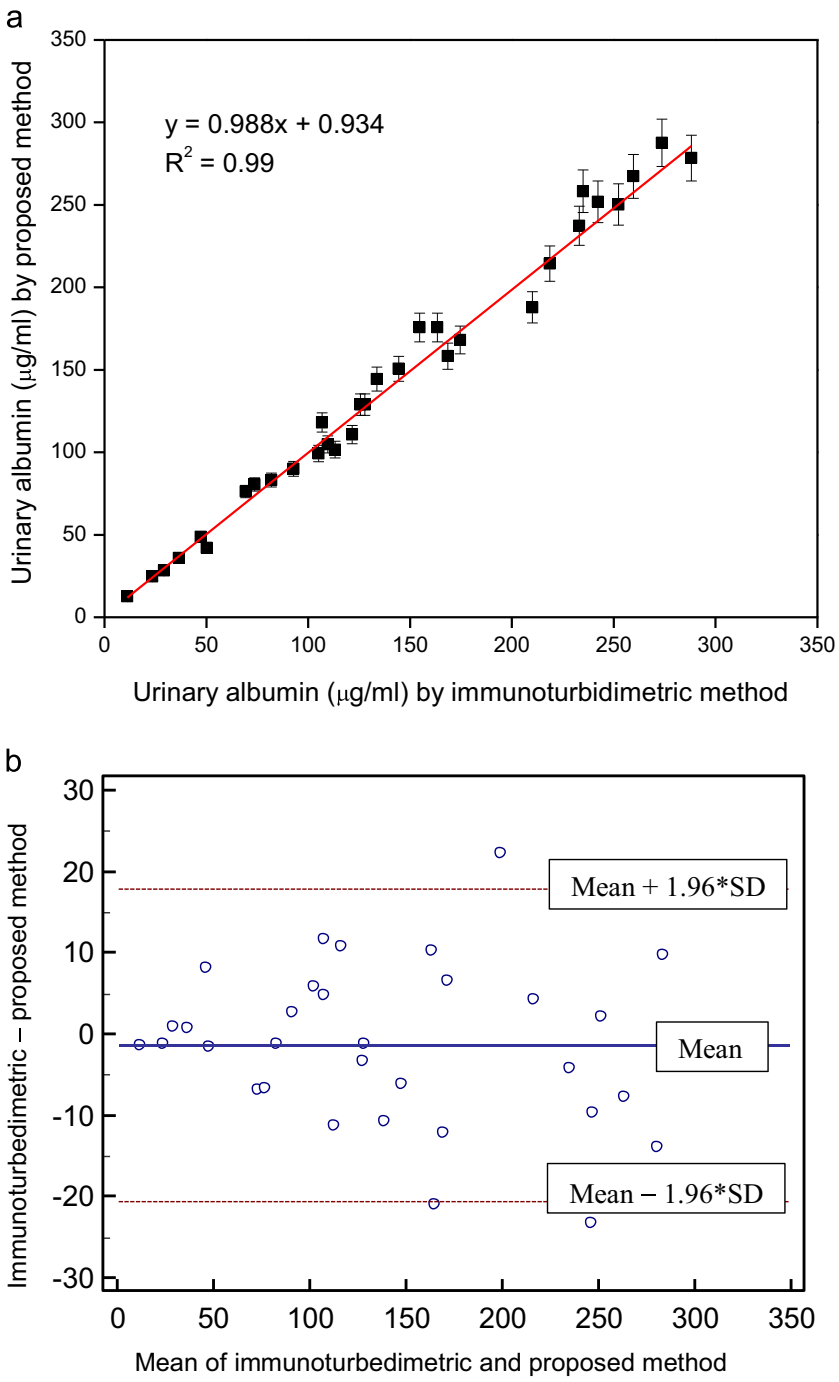

Fig. 6. Evaluation of the proposed immunosensor for clinical measurement of urinary albumin, using the immunoturbidimetric method as the gold standard. (a) Linear regression. (b) Bland–Altman plot.

Acknowledgments

This research was supported under Grant MOST 104-2221-E-008-073 and NSC 102-2221-E-008-103 by the Ministry of Science and Technology (formerly National Science Council), Taiwan. The authors thank Director Chi-Ching Chen, Department of Pathology and Laboratory Medicine, Landseed Hospital, Taiwan, for his valuable suggestions.

Appendix A. Supplementary material

Supplementary data associated with this article can be found in the online version at http://dx.doi.org/10.1016/j.bios.2015.11.002.

References

Aoyagi, S., Iwata, T., Miyasaka, T., Sakai, K., 2001. Anal. Chim. Acta 436, 103–108.
Bland, J.M., Altman, D.G., 1986. Lancet 327, 307–310.
Choi, S., Choi, E.Y., Kim, H.S., Oh, S.W., 2004. Clin. Chem. 50, 1052–1055.
Chugh, A., Bakris, G.L., 2007. J. Clin. Hypertens. 9, 196–200.
Comper, W.D., Jerums, G., Osicka, T.M., 2004. Clin. Biochem. 37, 105–111.
Datta, P., Dasgupta, A., 2009. J. Clin. Lab. Anal. 23, 314–318.
Dungchai, W., Chailapakul, O., Henry, C.S., 2009. Anal. Chem. 81, 5821–5826.
Fatoni, A., Numnuam, A., Kanatharana, P., Limbut, W., Thavarungkul, P., 2014. Analyst 139, 6160–6167.
Goyal, R.N., Gupta, V.K., Bachheti, N., 2007. Anal. Chim. Acta 597, 82–89.
Goyal, R.N., Gupta, V.K., Chatterjee, S., 2008. Talanta 76, 662–668.
Goyal, R.N., Gupta, V.K., Chatterjee, S., 2010. Sens. Actuators B: Chem. 149, 252–258.
Gupta, V.K., Jain, A.K., Maheshwari, G., Lang, H., Ishtaiwi, Z., 2006. Sens. Actuators B: Chem. 117, 99–106.

Jain, A.K., Gupta, V.K., Singh, L.P., Raisoni, J.R., 2006. Electrochim. Acta 51, 2547–2553.
Jain, R., Gupta, V.K., Jadon, N., Radhapyari, K., 2010. Anal. Biochem. 407, 79–88.
Kanyong, P., Pemberton, R.M., Jackson, S.K., Hart, J.P., 2012. Anal. Biochem. 428, 39–43.
Lai, T., Hou, Q., Yang, H., Luo, X., Xi, M., 2010. Acta Biochim. Biophys. Sin. 42, 787–792.
Li, H., Zhang, L.L., Cai, H.Y., Chen, X., Sun, J.H., Chao, Y.P., Cui, D.F., 2013. Key Eng. Mater. 562–565, 408–411.
Lin, Y., Lu, F., Tu, Y., Ren, Z., 2004. Nano Lett. 4, 191–195.
Marre, M., Claudel, J.P., Ciret, P., Luis, N., Suarez, L., Passa, P., 1987. Clin. Chem. 33, 209–213.
Moulder, J.F., Stickle, W.F., Sobol, P.E., Bomben, K.D., 1995. Handbook of X-ray Photoelectron Spectroscopy. Physical Electronics Division, Eden Prairie, Minnesota.
Newman, D.J., Mattock, M.B., Dawnay, A.B., Kerry, S., McGuire, A., Yaqoob, M., Hitman, G.A., Hawke, C., 2005. Health. Technol. Assess. 9, iii–vi, xiii-163.
Nie, Z., Nijhuis, C.A., Gong, J., Chen, X., Kumachev, A., Martinez, A.W., Narovlyansky, M., Whitesides, G.M., 2010. Lab Chip 10, 477–483.
Niu, X., Chen, C., Zhao, H., Tang, J., Li, Y., Lan, M., 2012. Electrochem. Commun. 22 (0), 170–173.
Omidfar, K., Dehdast, A., Zarei, H., Sourkohi, B.K., Larijani, B., 2011. Biosens. Bioelectron. 26, 4177–4183.
Petersen, P.H., Stockl, D., Blaabjerg, O., Pedersen, B., Birkemose, E., Thienpont, L., Lassen, J.F., Kjeldsen, J., 1997. Clin. Chem. 43, 2039–2046.
Polovina, M., Babić, B., Kaluderović, B., Dekanski, A., 1997. Carbon 35, 1047–1052.
Pournaghi-Azar, M.H., Ojani, R., 1995. Talanta 42, 1839–1848.
Ribera, M.C., Pascual, R., Orozco, D., Pérez Barba, C., Pedrera, V., Gil, V., 2006. Eur. J. Clin. Microbiol. Infect. Dis. 25, 389–393.
Sanagi, M.M., Ling, S.L., Nasir, Z., Hermawan, D., Ibrahim, W.A., Abu Naim, A., 2009. J. AOAC Int. 92, 1833–1838.
Thakkar, H., Newman, D.J., Holownia, P., Davey, C.L., Wang, C.C., Lloyd, J., Craig, A.R., Price, C.P., 1997. Clin. Chem. 43, 109–113.
Tholance, Y., Barcelos, G., Quadrio, I., Renaud, B., Dailler, F., Perret-Liaudet, A., 2011. Clin. Chim. Acta 412, 647–654.
Wang, T., Sherwood, P.M.A., 1994. Chem. Mater. 6, 788–795.
Watts, G.F., Bennett, J.E., Rowe, D.J., Morris, R.W., Gatling, W., Shaw, K.M., Polak, A., 1986. Clin. Chem. 32, 1544–1548.
Winograd, N., Blount, H.N., Kuwana, T., 1969. J. Phys. Chem.-US 73, 3456–3462.